The Malaysian Journal of ANALYTICAL SCIENCES ISSN 1394-2506

SELECTIVE SURFACE CHARACTERISTICS AND EXTRACTION PERFORMANCE OF A NITRO-GROUP EXPLOSIVE MOLECULARLY IMPRINTED POLYMER

(Karekter Permukaan yang Selektif dan Prestasi Pengekstrakan Kumpulan Nitro Peletup Polimer Molekul Tercetak)

Marinah Mohd Ariffin[1]*, Norhafiza Ilyana Yatim[1], Norhayati Mohd Tahir[1,2]

[1]*School of Marine and Environmental Sciences,*
[2]*Institute of Oceanography,*
Universiti Malaysia Terengganu, 21300 Kuala Terengganu, Malaysia

**Corresponding author: erin@umt.edu.my*

Received: 21 January 2015; Accepted: 5 April 2015

Abstract

A novel molecularly imprinted polymer (MIP) was synthesized as a highly selective and specific sorbent for solid phase extraction (SPE) of 2,4,6-trinitrotoluene (TNT). TNT-MIP was prepared by bulk polymerisation process using 2,4,6-trinitrotoluene (TNT) as template, methacrylic acid (MAA) as the functional monomer and ethylene glycol dimethylacrylate (EGDMA) as the cross-linker. Non-imprinted polymer (NIP) was prepared under the similar procedure but without the addition of template as a control polymer. Prior to analysis, the polymer monoliths were ground and sieved in the range of 25-38 µm before incorporated as SPE sorbent. The TNT-MIP and NIP performance validation were analysed by high performance liquid chromatography (HPLC) at 254 nm of UV detector. The limit of detection (LOD) and limit of quantitation (LOQ) range were 0.03-0.07 µg/mL and 0.05-0.11 µg/mL, respectively. The MIP showed excellent selectivity towards the template, TNT with percentage recovery and RSD value, 94.1±13.7 compared to TNT's metabolites, 4-amino-2,6-dinitrotoluene, 4-ADNT (31.7±27.2) and 2-amino-4,6-dinitrotoluene, 2-ADNT (41.2±6.1), respectively. The physical imprinting effect of MIP and NIP was characterized by using scanning electron microscopy (SEM) and Brunauer, Emmett and Teller (BET). Evaluation performance proved that the developed TNT-MIP was good in TNT selectivity and could be applied in real samples analysis.

Keywords: molecularly imprinted polymers, solid-phase extraction, 2,4,6-trinitrotoluene

Abstrak

Sebuah polimer molekul tercetak (MIP) baru telah disintesis sebagai pengerap yang sangat selektif dan khusus untuk pengekstrakan fasa pepejal (SPE) bagi 2,4,6- trinitrotoluena (TNT). TNT-MIP telah disediakan dengan proses pempolimeran pukal menggunakan 2,4,6- trinitrotoluena (TNT) sebagai templat, asid metakrilik (MAA) sebagai monomer, etilena glikol dimetilakrilat (EGDMA) sebagai pemaut silang. Polimer molekul tidak-tercetak (NIP) telah disediakan bawah prosedur yang sama tetapi tanpa tambahan templat sebagai polimer kawalan. Sebelum analisis, polimer dihancurkan dan ditapis dalam lingkungan 25-38 µm sebelum dijadikan sebagai penjerap SPE. Pengesanan prestasi TNT-MIP dan NIP dianalisis oleh kromatografi cecair berprestasi tinggi (HPLC) pada 254 nm pengesan UV. Had pengesanan (LOD) dan had kuantitatif (LOQ) adalah, 0.03-0.07 µg/mL dan 0.05-0.11 µg/mL masing-masing . MIP menunjukkan pemilihan yang cemerlang ke arah templat, TNT dengan peratus pengembalian dan nilai RSD , 94.1 ± 13.7 berbanding metabolit TNT , 4-amina-2,6-dinitrotoluena , 4-ADNT (31.7 ± 27.2) dan 2-amina-4, 6-dinitrotoluena, 2-ADNT (41.2 ± 6.1). Kesan fizikal pencetakan MIP dan NIP dicirikan dengan menggunakan mikroskop imbasan elektron (SEM) dan Brunauer, Emmett dan Teller (BET). Penilaian prestasi membuktikan bahawa TNT-MIP yang dibangunkan bagus digunakan TNT pemilihan dan boleh digunakan dalam analisis sampel sebenar.

Kata kunci: polimer molekul tercetak, pengekstrakkan fasa pepejal, 2,4,6-trinitrotoluena

Introduction

The detection of nitroaromatic explosives has grown rapidly due to the dire need for public security and environmental protection. In this study, focus towards the analysis of 2,4,6-trinitrotoluene (TNT) was discussed due to it extends application in military, industries, mining and agricultural activities. This compound has good chemical and thermal stability, low volatility and moderate toxicity compared to other hazardous explosives. TNT poisoning can lead to severe and chronic diseases, such as aplastic anemia or toxic jaundice. In aplastic anemia, which is often fatal, the blood-forming organs fail to function, resulting in progressive loss of blood elements. Toxic jaundice indicates that the liver is severely damaged. Less serious diseases resulting from TNT intoxication include headache, cataract, dermatitis, gastritis, cyanosis, and disorders of the nervous system. On top of that, the EPA (Environmental Protection Agency) has determined that TNT is a possible human carcinogen [1]. TNT occurance in soil was normally due to washdown operation or explosion process. This process will eventually lead to soil contamination as TNT is immobile once its entered the environment.

A good analytical technique include good screening, clean-up and extraction is required for the analysis of low concentarion of TNT in environmental samples. Previous findings by Trammell *et al.* (2008) and Lordel *et al.*, (2010) discussed on the succesful application of Solid-phase Extraction (SPE) technique of aromatic explosives [2,3]. In order to obtain a better selective technique of extraction, a specific SPE adsorbent should be designed towards target analytes.

This research utilized a molecular imprinting technology in order to create specific recognition sites for the targeted TNT in synthetic polymers. In general, the imprinting effect within polymer monolith is created by three-dimensional polymeric networks involving the interaction of the template with surrounding functional monomers and the cross-linked matrix [4,5]. After the polymerization process, template was removed by appropriate treatment, which leaves behind its imprinted cavities and commonly known as binding sites. The binding sites can rebind the template from different media with appreciable selectivity [6]. The imprinted polymer then employed as an adsorbent for SPE for the extraction and quantification of 2,4,6-trinitrotoluene (TNT). The extraction performance of developed TNT-Molecularly Imprinted SPE (TNT-MISPE) was evaluated and its physical properties were characterized by SEM, BET and FTIR.

Materials and Methods

Materials and Chemicals

Liquid form of analytical grade 2,4,6-trinitrotoluene (TNT) was purchased from Supelco (Bellefonte, USA) and the solid form of industrial grade TNT was obtained from Science and Technology Research Institute of Defence (STRIDE) (Batu Arang, Malaysia). 2-amino-4,6-dinitrotoluene (2-ADNT) and 4-amino-2,6-dinitrotoluene (4-ADNT) were obtained from AccuStandard (New Haven, CT, USA). Synthesis grade methyl acrylic acid (MAA, ≥99%) and ethylene glycol dimethacrylate (EGDMA, ≥98%) were purchased from Merck (Darmstadt, Germany). Both these chemicals were purified prior to use by passing through a short column of alumina oxide from R&M Chemical (Essex, UK) in order to remove the stabilizer (2%, hydroquinone monomethyl ether) (EPA, 1996). 2,2‘-azobisisobutyronitrile (AIBN) was purchased from R&M Chemical (Essex, UK). The following commercial chemicals of reagent-grade were used in the synthesis- chloroform, methanol, acetonitrile, acetone and acetic acid, which were purchased from Merck (Darmstadt, Germany).

The SPE manifold set was purchased from Supelco (Bellefonte, USA). The empty, 1 mL polypropylene SPE cartridges and frits (20 μm mean pore size) were supplied by Phenomenex (Torrance, CA, USA). The commercial strata-X SPE tubes (30 mg/1 mL) Phenomenex (Torrance, CA, USA) were used for analyzing samples. Sample extraction was done by using compact CF16RX11, Hitachi high-speed micro centrifuge (Chiyoda, Tokyo, Japan).

Synthesization of Molecularly Imprinted Polymers

The molecular imprinted polymer, MIP was synthesized by dissolving 1 mmol (0.1318 g) of template, 2,4,6-trinitrotoluene, TNT, 4 mmol (0.1968 mL) of monomer, methylacrylic acid, MAA in 4.9 mL chloroform as a porogen in a thick walled glass tube. After standing the mixture for 5 minute, 20 mmol (2.2662 mL) of the cross-linker, ethylene glycol dimethylacrylate, EGDMA was added, followed by addition 0.1258 g of 2,2‘-

azobisisobutyronitrile, AIBN to initiate the polymerization process. The mixture was then sparged with oxygen-free nitrogen while cooling in an ice bath for a few minutes to remove the oxygen. This sealed glass tube was transferred into a water bath at a temperature of 60 ºC for 24 hours to cure the polymer. The non-imprinted polymer (NIP) was also prepared in the same procedure but without the addition of template. Then, MIP and NIP monoliths were crushed by mechanically grounding and wet-sieved using acetone to deliver polymers in varying size (in a range of 25-38 µm). After 24 hours of extensive washing through Soxhlet extraction with chloroform to discard the template from the MIP, the polymer particles were then dried in a vacuum oven at temperature of 60ºC for 24 hours prior to use.

In this study, MAA was preferred as functional monomer compared to other carboxylic acid according to its special chemical properties such as compact and structure is stabilized by hydrogen bonding which formed from poly-MAA. Subsequently the methyl group of MAA is prevalent produces hydrophobic effect [7]. Based on the previous finding, the nature of MAA can stabilize the conformational behavior of PMAA as it were ionized in aqueous solution [8]. Therefore, in poor solvents, the poly-MAA and the cross-linker, EGDMA can assemble networks strongly.

Molecularly Imprinted Polymer Solid Phase Extraction Protocols

MISPE and NISPE catridges were separately packed with 20 mg of MIP and NIP particles (25-38 µm) in empty 1 mL polypropylene SPE cartridges. First, a 20 µm polyethylene frit was inserted into an empty 1 mL polypropylene SPE cartridge. Then, 20 mg of MIP was slurried with acetone into the cartridge. The cartridge was subjected to vacuum for ~30 s before inserting the second frit on top of the sorbent. The MISPE-cartridges were treated by washing it with 1 ml of methanol–acetic acid (70:30, v/v) for few times to remove the bound and unbound of template before applying the cartridge in accordance with MISPE protocols. Each washing eluent was collected, evaporated to dryness by gentle blowing nitrogen gas at room temperature and reconstituted with 0.3 mL of the mobile phase prior to analysis by HPLC. In between the treatment series, the MIP sorbent was allowed to dry.

MISPE Performance Validation

The linearity and determination of the LOD and LOQ of MISPE and NISPE are performed by preparing a standard stock solution of TNT and its metabolites at a concentration of 100 µg/mL in methanol. Standard 2,4,6-trinitrotoluene, TNT, 2-amino-4,6-dinitrotoluene, 2-ADNT and 4-amino-2,6-dinitrotoluene, 4-ADNT spiking at concentrations of 0.5, 0.25, 0.125, 0.0625, 0.0313, 0.0156, and 0.0078 µg/mL were extracted by MISPE protocols and analyzed by HPLC-UV at 254 nm. Calibration curves with linear regressions were prepared by plotting the peak area value of standards against the spiked analyte concentrations. LOD and LOQ were experimentally estimated for every single analyte of TNT and its metabolites from the injection of standard solutions serially diluted until the signal-to-noise ratio [9].

Recovery Study

For recovery study, the mixture of nitroaromatic compounds are passed through the optimized MISPE protocols and the percent mean recovery and percent relative standard deviation (RSD) were calculated for the each compound. The extraction method for both MISPE and NISPE were carried out according to the previously established protocol. First, the cartridges were conditioned with 1 mL of methanol followed with loading of 300 µL, of 0.05 µg/mL of mix standard which composed of TNT, 2-ADNT and 4-ADNT. Then the cartridges were washed with 300 µL of deionised water:methanol (80:20, v/v) to discard unbound analytes. The retained analytes in the cartridge were eluted with 500 µL of acetonitrile for twice to extract all the analytes. The eluent was blown dry by stream of nitrogen gas at room temperature. It was then reconstituted with 0.3 mL of methanol for HPLC analysis. The recovery was calculated by comparing the ratio of peak obtained from extracted samples to the peak area of the same concentration of pure standards directly analyzed by HPLC.

Real Sample Analysis

1 mL of the extracted soil sample was passed through the MISPE and NISPE cartridge using the optimized MISPE protocols. For commercial SPE (STRATA-X), the sample extraction followed SPE protocol provided by the supplier. For conditioning, 0.5 mL of methanol was used, followed by 0.5 mL of water to equilibrate the SPE. Then, after loading the sample, SPE was washed with 0.5 ml of methanol:water (10:90, v/v) and dried under full vacuum

for 10 minutes before eluting the sample with 0.5 ml of methanol. All the samples eluted from MISPE, NISPE and Strata-X SPE were evaporated to dryness with nitrogen gas and reconstituted with 0.5 mL of methanol prior to HPLC analysis. The nitroaromatic compounds detected were calculated based on the plotted calibration curve of known concentration of analytes.

Physical Characterization of Polymers

Physical characterizations of the polymers were carried out using scanning electron microscopy (SEM) (JEOL model JSM-6360 LA) and Brunauer, Emmett and Teller (BET) Autosorb 1-C instrument from Quantachrome (Florida). The surface morphology of MIPs and NIPs polymer monolith were observed under the JSM-6360 LA JEOL SEM. Thin layer of these polymer were coated with gold (Au) prior to being observed by the SEM. Gold coating produced fine images depicting the polymer surfaces at high magnification and protects the polymer surface from the electron's beam with kinetic energies of about 1-25 kV. The surface area analysis was performed by using the Autosorb 1-C instrument from Quantochrome. The nitrogen adsorption and desorption process was measured at 77 K and the samples were out-gassed in a vacuum at 110°C for 10 h prior to analysis. The BET area of the polymer materials (SBET) was calculated from the adsorption data using 0.162 nm^2 as the molecular cross-sectional area for adsorbed nitrogen molecules. The Barret–Joyner–Halenda (BJH) method was used to calculate the pore size distribution by applying the Kelvin equation under assumption of cylindrical pores. The infrared spectrum of polymer monoliths were done by using the potassium bromide (KBr) pellet technique and recorded in the range of 400–4000 cm^{-1}. Gaussian 09 software package was adapted to theoretically estimate the total radius of the template and hydrogen bonds in developed TNT-MIP. These data were then compared to the experimental data obtained in the latter stage. This software employed the basic set (B3LYP 6-31G) with Monte-Carlo calculations to study the optimized structures of TNT, 2-ADNT and 4-ADNT [10]. Chromatographic investigation was performed on HPLC-UV Shimadzu equipped with SCL autosampler and variable-wavelength UV as detector. 254 nm was selected as the maximum absorption wavelength of TNT. C18 Synergy Hydro-RP HPLC column supplied by Phenomenex (250 mm L x 4.6 mm i.d, 4 µm particle size) was employed for chromatographic separation of TNT and its metabolites. The mobile phase used in the chromatographic separation consists of a binary mixture of solvents A (water) and B (methanol) at a constant flow rate of 1.0 mL min-1. Mobile phase gradient program was used with the elution start with 55% (B) which was maintained for 2 minute, followed by a 20 minute of linear gradient to 65% (B) and 2 minute linear gradient back to 55% (B).

Results and Discussion

MISPE performance validation

LOD and LOQ of MISPE were summarized in Table 1. The correlation coefficients (r) of the method calibration curves were ≥ 0.993 for all analytes.The regression analysis between peak areas of nitroaromatic compounds versus concentration showed satisfactory linearity in the range of 0.0078-0.5 µg/mL. The proposed MISPE protocol provides a satisfactory and good LOD and LOQ for the simultaneous detection of TNT and its metabolites in the soil sample. Figure 1 shows these mix compounds was successfully separated by using the Phenomenex HPLC column and detection at a wavelength of 254 nm by UV detector.

Table 1. The LOD and LOQ values of the TNT and its metabolites using MISPE

Analyte	LOD[a] (µg mL^{-1})	LOQ[b] (µg mL^{-1})	r
2,4,6-trinitrotoluene (TNT)	0.028	0.047	0.9979
4-Amino-2,6-dinitrotoluene(4-ADNT)	0.034	0.057	0.9976
2-Amino-4,6-dinitrotoluene(2-ADNT)	0.066	0.110	0.9932

[a] Limit of detection . [b] Limit of Quantitation

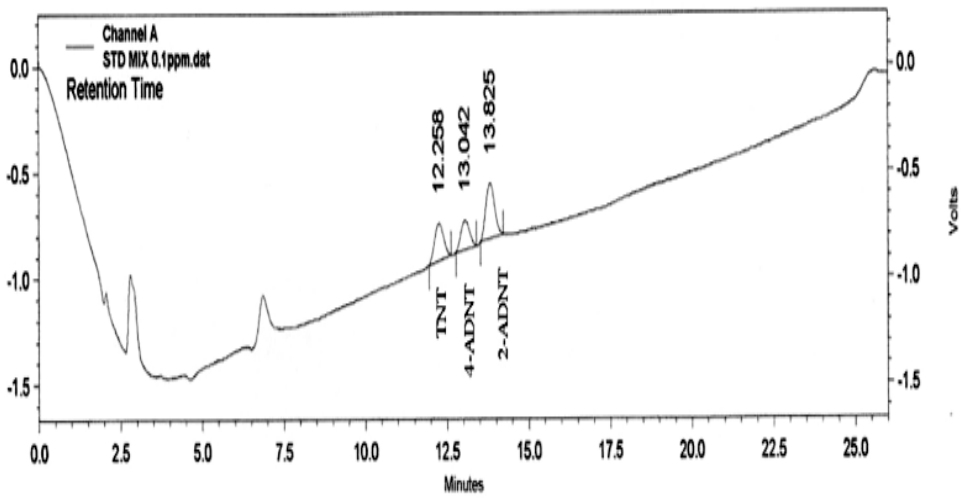

Figure 1. Chromatogram of the selected nitroaromatic compounds standard mixture at 0.1 µg/mL (ppm). Conditions: C18 Synergy Hydro-RP HPLC column (250 mm × 4.6 mm i.d, 4 µm particle size), methanol:deionised water, gradient elution 55:45 solvent for 2 minutes, gradient elution 55:45 to 75:25 in 20 minutes and gradient elution dropped to 55:45 in 3 minutes and maintained for 1 minute.

Recovery study

Recovery study has been performed for selected nitroaromatic compounds and the result obtain has tabulated in Table 2. Table 2 shows the MIP recovered a high percentage of TNT, followed by 2-ADNT and 4-ADNT. The extraction recoveries obtained were approximately 31.7% and 41.2% for the 4-ADNT and the 2-ADNT, respectively.

Table 2. Mean (%) recovery and (%) RSD of MISPE and NISPE for nitroaromatic compounds (n=4)

Analyte	% Recovery (% RSD)	
	MISPE	NISPE
TNT	94.1 (13.7)	72.1 (7.3)
4-ADNT	31.7 (27.2)	36.1 (31.8)
2-ADNT	41.2 (6.1)	43.8 (12.9)

High RSD values of 4-ADNT for MISPE and NISPE indicated less interaction between this analyte towards the polymer sorbent. Its recovery also displayed the worst performance of detection in MISPE (31.7%) and NISPE (36.1%). Low RSD value of other TNT metabolites (2-ADNT) for MISPE and NISPE showed that this analyte is a competitor to TNT as similarity in structure. The TNT recovery of MISPE showed satisfactory (94.1%) value compared to its metabolites. This proves that the recognition properties of MISPE had successfully extracted towards to the target analyte, TNT. NISPE also presented the bounded nitroaromatic compounds to the surface of non-imprinted polymer related to the excess free functional monomers in synthesizing polymers process that might lead to strong interactions to non-specific sites [11].

Real sample analysis

In this study, the real sample analysis has been performed using quarry sample and control sample from Kenyir area. From the analysis of 1 g of quarry soil sample the concentration of TNT found was 0.06 µg/mL and 0.07 µg/mL when extracted using imprinted polymer (MISPE) and STRATA-X commercial SPE, respectively. Table 3 shows the summary of the sample extractions for TNT and its two metabolites.

Table 3. Real sample analysis of soil from polluted (quarry) and unpolluted site (Kenyir) by using MISPE, NISPE and STRATA-X SPE

Nitroaromatic compounds (µg/ml)	Soil (Quarry)			Soil (Kenyir)		
	MISPE	NISPE	STRATA-X	MISPE	NISPE	STRATA-X
TNT	0.060	0.041	0.074	ND	ND	ND
4-ADNT	ND	ND	ND	ND	ND	ND
2-ADNT	ND	ND	ND	ND	ND	ND

**M=MISPE, N=NISPE, S=SRATA-X, ND=not detected*

Even the commercial SPE performed better sensitivity towards TNT, the developed MISPE was more convenient due to its reusability, cost-effectiveness, less solvent usage and less time consumed for the analysis procedure. Interestingly, this selective and economical technique can be utilized for monitoring TNT levels in related fields, in order to ensure the welfare of health workers and local residents.

Physical Characterizations by of molecularly imprinted polymer

The scanning electron microscopy (SEM) was performed to study the characterization of surface morphology of MIPs and NIPs particles. The Figure 2 (a) and (b) of SEM images displayed by the MIP and NIP shown no significant difference in morphological structure. The result obtained was agreed with previous findings, that imprinted and non-imprinted polymers were mostly depicted non-porous surfaces when non-polar solvent was used as the porogen in the polymerization process [12].

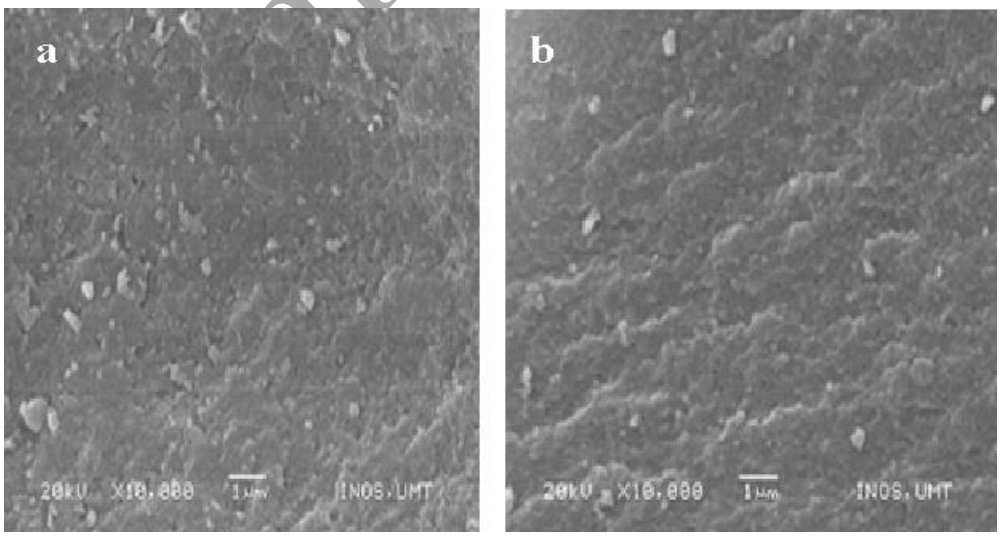

Figure 2. SEM micrographs of (a) MIP and (b) NIP surfaces (magnification x 10,000).

Figure 3 shows the nitrogen adsorption and desorption isotherms of polymer monoliths of MIP and NIP. The physisorption isotherms show to be Type IV, which indicated the existence of mesoporosity with high energy of adsorption cavities in MIP and NIP polymer monoliths, respectively. Characteristics of Type IV were the presence of its hysteresis loop which is appeared related to the capillary condensation occurred in the mesopore structures. MIP tends to exhibit a hysteresis loop of a Type H2. This Type H2 indicates that its pores have a narrow neck with wide bodies, generally known as 'ink-bottle-shapes' pores. This characteristic confirms the formation of cavities within the monolith. This loop displays a different mechanism for the condensation and evaporation process that occured in the pore cavities. In Figure 4.2 (b), the NIP shows a hysteresis loop of a Type H4, referred to the presence of narrow slit-like pores and verified that there was no imprinting effects of the template[13,14].

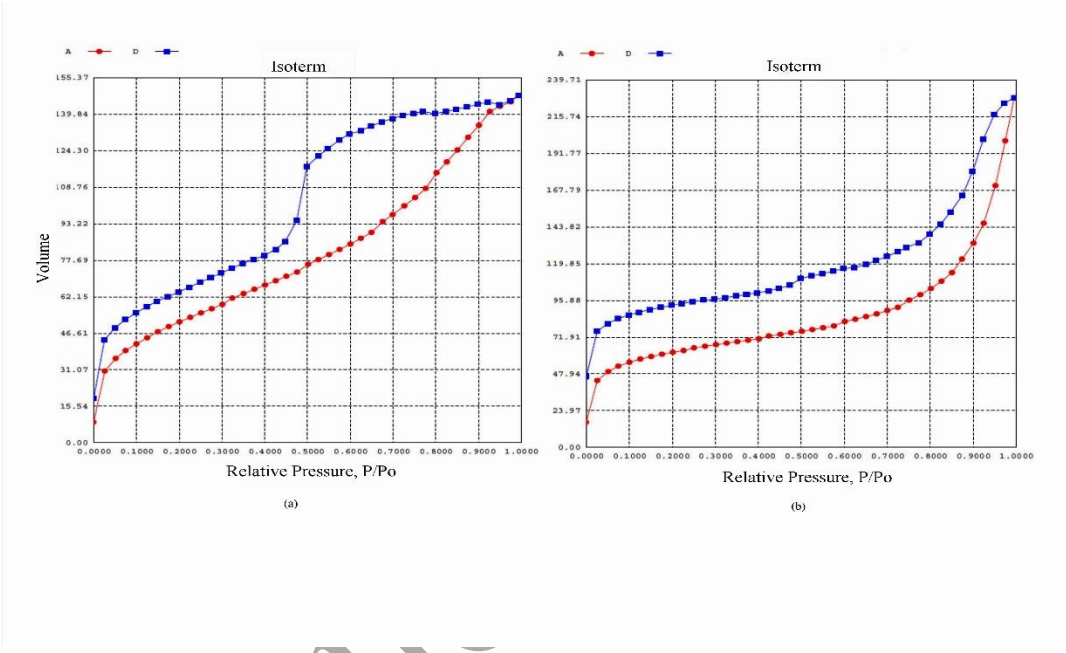

Figure 3. Nitrogen adsorption-desorption isotherms of polymer MIP (a) and NIP (b). Volume (cc g^{-1}) versus relative pressure (P/Po). —●— = adsorption, —▮— = desorption.

In the context of physisorption, it is practical to classify pores based on their sizes. Therefore, Table 3 indicates that MIP was classified as mesopores (2–50 nm) and NIP as micropores (< 2 nm). Surface area and pore volume of NIP were showed higher value than MIP due to its narrow slit-like pores (Table 4). The polymer with smaller pores is normally produced when the phase separation occurred during the polymerisation process [15].

Table 4. Surface area and pore analysis of MIP and NIP by nitrogen sorption porosity.

Polymer	**BET surface area, S_{BET} (m^2/g)[a]**	**External surface area, S_t (m^2/g)[b]**	**Pore volume (cc/g)[c]**	**Pore diameter (Å)[d]**
MIP	186.7	133.8	0.2864	39.32
NIP	206.3	137.7	0.3828	8.581

[a] Surface area from multipoint BET value on a eleven-point linear plot,[b]External surface area obtained from the *t*-plot, [c]BJH method cumulative desorption pore volume, [d]BJH method desorption pore diameter

Figure 4 displays the pore size distribution curves from desorption of pore diameters and apertures of MIP (a) and NIP (b). The condensation and evaporation processes occurred at relative pressures related by the Kelvin equation to the diameters of pores and openings, correspondingly. During the adsorption process, the gas condensates inside the pores at particular pressure values depending on the cavity diameters but, during the desorption process, evaporation starts from the meniscus at the pore's entrance when the relative pressure corresponds to the aperture size.The cavities created in MIP was showed well defined maxima homogenous pore openings in a range of pore diameters (35.03-41.77 Å) or (3.50-4.17 nm); (0.1082-0.2232 cc/g) Figure 4 (a) was classified as in the mesopore region (2nm<pore diameter<50nm) [16]. Figure 4 (b) shows that the heterogenous opening in size and the narrow slit-like pores maxima at (35-41.6 Å) or (3.5-4.16 nm) with pore volume (0.1508-0.1703 cc/g). The higher pore diameter of MIPs were displayed the higher imprinting effect of templates [17].

The porogen, as a pore-forming agent, is definitely influence the polymer morphology. It provides a medium for solvation of growing polymer chains, which contributes to the pore structure mechanisms [18]. In addition, a thermodynamically good solvent tends to fabricate a polymer with well-develope pore structure with a high specific area. The surface area of polymers is strongly controll by the amount of porogen and the concentration of cross-linkers. Increase amount of porogen and cross-linkers, will lead to the production polymers with high surface areas [19,20,21]. Previous studies have shown that the application of chloroform as a porogen in the complexation of functional monomer and template has produced less or no porosity of the surface areas. The polymer made from this porogen is solvated to a high degree and allowed the fast diffusion of substrates without requiring porosity property [22].

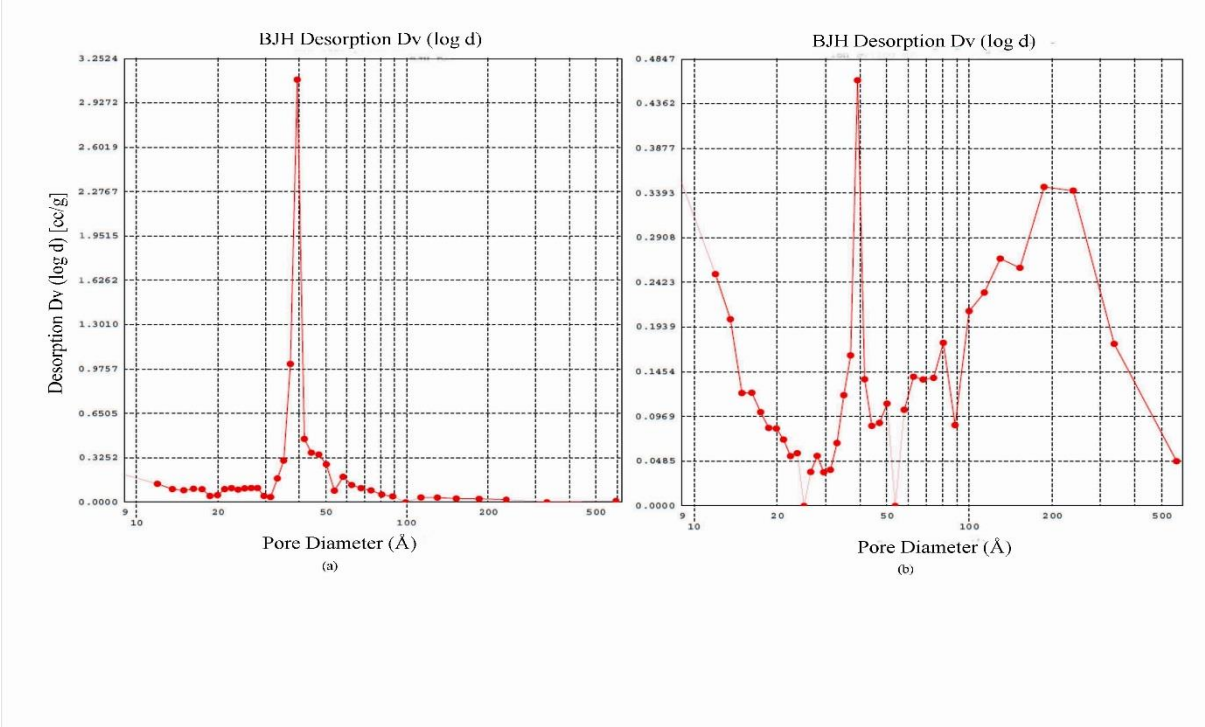

Figure 4. Pore size distribution curves were plotted from the BJH desorption for (a) molecular imprinted polymer (MIP) materials and (b) non-imprinted polymer (NIP) materials.

The structure of TNT and its metabolites were also analyzed by the Gaussian software program and used the basis set, B3LYP 6-31G, to study the molecular simulation of the template structure in terms of cavity size that have been

created in the polymer monoliths. To interpret the experimental data, the Monte Carlo calculation method was applied. Equation 1 displays the theoretical calculation of the approximate radius cavities created in MIP [23].

$$\text{Radius cavities created} = (\text{radius} + \text{hydrogen bonding}^*)\ \text{Å} \quad (1)$$

*hydrogen bonding = 1.937Å

Table 5. Summary of Gaussian data for TNT, 4-ADNT and 2-ADNT by the Monte Carlo calculation method

Analyte	Radius (r, Å)	Radius cavities (r, Å)	Molar volume ($cm^3\ mol^{-1}$)	Dipole moment (μ, Debye)
TNT	4.52	6.457	123.188	1.5945
4-ADNT	4.44	6.377	123.9	4.7925
2-ADNT	4.53	6.467	115.479	6.3621

The approximate radius cavity created after the template (TNT) removal in MIP cavities was about 6.457 Å (Table 5). The radius cavities created were represented by the actual radius of analytes and the expected hydrogen bonding produced. From the values of actual radius cavities, other metabolites such as 2-ADNT and 4-ADNT can also fitted in the cavities imprinted by TNT, as their radius is quite close to TNT. The value of estimate size of cavities created in MIP by Gaussian analysis shows smaller than the the value of cavity size analyzed by BET (35.03-41.77Å)(Figure 4 (a)). This corresponding to the different condition of BET analysis which was conducted in dry state of the polymer. However, for the rebinding step, the process occurred in the solvent and probably the polymer would swollen and the cavities size decreased, therefore it fitted into the TNT size. Figure 5 illustrated the optimized structures of TNT and its metabolite compounds from the Gaussian analysis.

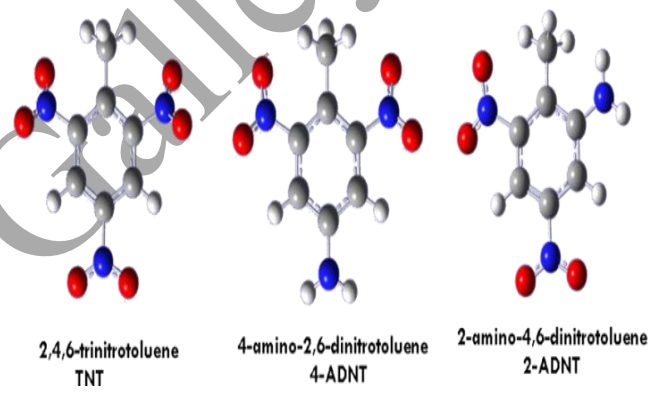

Figure 5. Optimization of molecule structure by Gaussian using B3LYP 6-31G as the basis set showing grey-carbon atoms, light grey-hydrogen atoms, blue-nitrogen atoms and red-oxygen atoms.

The infrared spectrum of TNT imprinted polymer (MIP) and non-imprinted polymer (NIP) were illustrated in Figure 6. Previous studies have revealed that the interaction involved is between TNT and the monomer, MAA are based on hydrogen bonding. The interaction between (nitro group-NO_2) and the MAA (carboxyl group–COOH) can be observed by the different intensity of percentage transmittance for both spectra MIP and NIP.

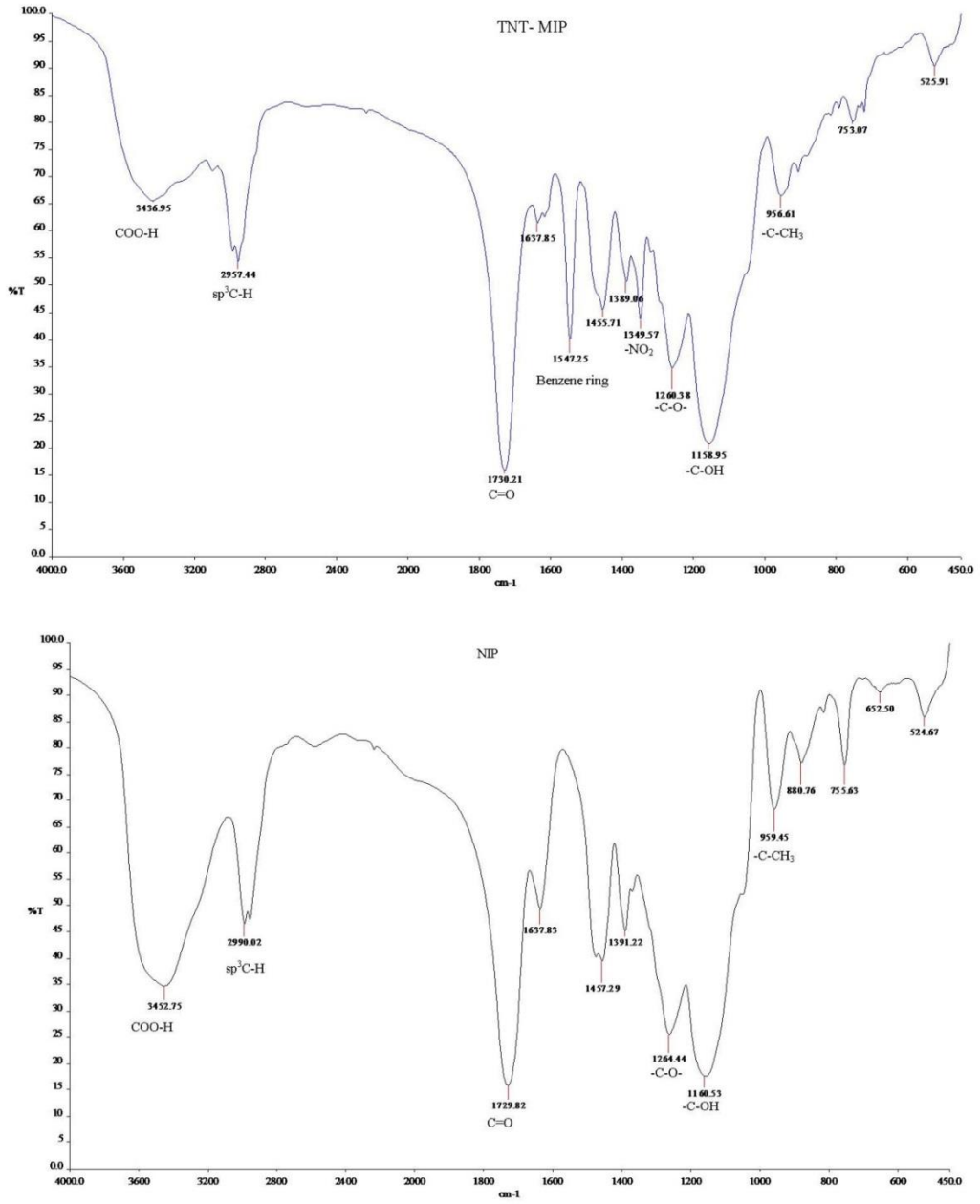

Figure 6. Infrared spectra (KBr pellet) of TNT imprinted polymer (MIP) (above) and non-imprinted polymer (NIP) (below) using chloroform as a porogen.

Spectrums of MIP and NIP in Figure 6 showed the presence of a carboxyl group by the intense absorbance from 3500 to 2500 cm^{-1} were observed which corresponds to the –O-H stretch of the carboxyl group. This broad band is highly characteristic of carboxylic acid and follow the presence of a strong peak in the 1730 to 1680 cm^{-1} region, which is assigned to the C=O stretching absorption in the samples.

MIP spectra showed the extremely broad peak at 3436.95 cm^{-1} which indicated the presence of hydrogen bonds. The intermolecular hydrogen bond between TNT and polymer also contributed to this broadening peak. The NIP spectra depicted a strong and sharp peak at 3452.75 cm^{-1}, showed the carboxylic acid COO-H and non-hydrogen bonding [24]. The lower intensity of C-OH bonding of MIP at 1158.95 cm^{-1} compare to NIP (1160.53 cm^{-1}) was attributed to the hydrogen bond forming between the template and the monomer. The band at 1637.83 cm^{-1} and 959.45 cm^{-1} of NIP gave information about the amount of unreacted double bonds in the polymer material.

The peak of the benzene ring deformation at a frequency of 1547.25 cm^{-1} and the N-O stretching at 1349.57 cm^{-1} was notified the bounded template in MIP spectrum [25]. However, the presence of other peaks is related to the chemical information of polymer chain build-up from MAA and EGDMA, which are the monomer and cross-linker, respectively. The result suggested that hydrogen bonding was successfully formed between the template and the monomer as predicted in the theory.

Conclusion

In this study, molecularly imprinted polymer was successfully prepared for TNT detection by using the non-covalent approach. Based on the functional groups on the template molecule, an appropriate functional monomer, methylacrylic acid (MAA), was selected to form the template-monomer complex. Physical and chemical characterization analysis by using the SEM, BET, FTIR and computational chemistry (Gaussian software) had provided evidence of chemical interaction, surface morphology and cavities of polymer monoliths, which are the key to fundamental imprinting studies. The binding results for the template molecule and its metabolite molecules showed that the MIPs possess the predesigned affinity and selectivity and effectively applied in real sample analysis.

For the future works, this finding can be commercialized in industrial scale by improving the polymerization technique to increase the yield of MIPs, and application of advanced device formats such as LC-MS to improve the sample evaluation in terms of speed and sensitivity. In addition, computer-aided approach promises to replace tedious trial and error methods with fast simulation based on chemical modeling in order to obtain better selectivity of MIPs by choosing the best combination of templates, cross-linkers, monomers and porogens.

Acknowledgement

We gratefully acknowledge the Ministry of High Education of Malaysia (MOHE) under Fundamental Research Grant Scheme (FRGS No. 59154) for funding this project entirely. Our institution, University Malaysia Terengganu (UMT) thankfully acknowledged for providing facilities in our lab works.

References

1. Yinon, J. (1999). Environmental detection explosives. Forensic and Environmental Detections of Explosives, pp 186-219. New York: John Wiley & Sons, Ltd
2. Trammell, S. A., Zeinall, M., Melde, B. J., Charles, P. T, Velez, F. L., Dinderman, M. A., Kusterback, A. and Markowitz, M. A. (2008). Organosilicas as Preconcentration Materials for the Electrochemical Detection of Trinitrotoluene. *Analytical Chemistry* 80: 4627–4633.
3. Lordel, S. Chapuis-Hugon, F., Eudes, V., and Pichon, V. (2010). Development of imprinted materials for the selective extraction of nitroaromatic explosives. *Journal of Chromatography A* 1217: 6674–6680.
4. Tamayo, F. G., Turiel, E., and Martin-Esteban, A. (2007). Review: Molecularly imprinted polymers for solid-phase extraction and solid-phase microextraction: Recent developments and future trends. *Journal of Chromatography A* (1152): 32–40.
5. Poma, A., Turner, A. P. F., and Piletsky, S. A. (2010). Advances in the manufacture of MIP nanoparticles, *Trends in Biotechnology* 28(12): 629-637.

6. Tóth, B., Pap, T., Horvath, V., and Horvai, G. (2007). Which molecularly imprinted polymer is better?. *Analytica Chimica Acta* 591: 17–21.
7. Pomogailo, A. D., Dzhardimalieva, G. I., and Kestelman, V. N. (2010) Macromolecular Metal Carboxylates and Their Nanocomposites. *Springer Series in Materials Science* 138, 7-25.
8. Sulatha, M. S., and Natarajan, U. (2011) Origin of the Difference in Structural Behavior of Poly(acrylic acid) and Poly(methacrylic acid) in Aqueous Solution Discerned by Explicit-Solvent Explicit-Ion MD Simulations. *Industrial Engineering and Chemistry Research* 50 (21):11785–11796.
9. Miller, J. N., and Miller, J. C. (2000). Calibration methods in instrumental analysis: regression and correlation. In Statistics and chemometrics for analytical chemistry, 4th edition, pp 107-147. England: Prentice Hall.
10. Nicholls, I. A., Andersson, H. S., Charlton, C., Henschel, H., Karlsson, B. C. G., Karlsson, J. G., O'Mahony, J., Rosengren, A. M., Rosengren, K. J. and Wikman, S. (2009). Review: Theoretical and computational strategies for rational molecularly imprinted polymer design. *Biosensors and Bioelectronics* 25: 543–552.
11. Gonz´alez, G. P., Hernando, P. F., Alegr´ia, J. S. D. (2006). A morphological study of molecularly imprinted polymers using the scanning electron microscope. Analytica Chimica Acta 557: 179–183.
12. Haginaka, J., Tabo, H., Kagawa, H. (2008). Uniformly sized molecularly imprinted polymers for d-chlorpheniramine: Influence of a porogen on their morphology and enantioselectivity. *Journal of Pharmaceutical and Biomedical Analysis* 46: 877–881.
13. Condon, J. B. (2006). Surface Area and Porosity Determination by Physisorption: Measurement and Theory. Elsevier. 1-27.
14. Sing, K. S. W., Everett, D. H., Haul, R. A. W., Moscou, L., Pierotti, R. A., Rouquérol, J., and Siemieniewska, T. (1985). Reporting Physisorption Data For Gas/Solid Systems with Special Reference to the Determination of Surface Area and Porosity. *Pure & Applied Chemistry* 57(4): 603—619.
15. Qi, P., Wang, J., Wang, L., Li, Y., Jin, J., Su, F., Tian, Y., and Chen, J. (2010). Molecularly imprinted polymers synthesized via semi-covalent imprinting with sacrificial spacer for imprint ing phenols. Polymer 51: 5417-5423.
16. Barrett, E. P., Joyner, L. G., and Halenda, P. P. (1951). The Determination of Pore Volume and Area Distributions in Porous Substances. I. Computations from Nitrogen Isotherms. The Volume and Area Distributions In Porous *Substances* 73: 373-380.
17. Sellergen, B., and Shea, K. J. (1993). Influence of polymer morphology on the ability of imprinted network polymers to resolve enantiomers. Journal of Chromatography 635: 31-49.
18. Masquè, N., Marcè, R. M., and Borrull, F. (2001). Molecularly imprinted polymers: new tailor-made materials for selective solid-phase extraction. *Trends in Analytical Chemistry* 20(9): 477-486.
19. Sellergen, B., and Hall, A. J. (2001). Fundamental aspects on the synthesis and characterisation of imprinted network polymers. In Molecularly imprinted polymers. Man-made mimics of antibodies and their applications in analytical chemistry: Techniques and instrumentation in analytical chemistry Volume 23, ed. B. Sellergen, pp 21-57. Amsterdam: Elsevier.
20. Cormack, P. A. G., and Elorza, A. Z. (2004). Review: Molecularly imprinted polymers: synthesis and characterization. *Journal of Chromatography B* 804: 173–182.
21. Dong, W., Yan, M., Liu, Z., Wu, G., and Li, Y. (2007). Effects of solvents on the adsorption selectivity of molecularly imprinted polymers: Molecular simulation and experimental validation. *Separation and Purification Technology* 53: 183–188.
22. Spivak, D. (2005). Optimization, evaluation, and characterization of molecularly imprinted polymers. Advanced Drug Delivery Reviews 57: 1779– 1794.
23. Saloni, J., Lipkowski, P., Dasary, S. S. R., Anjaneyulu, Y., Yu, H. and Jr, G. H. (2011). Theoretical study of molecular interactions of TNT, acrylic acid, and ethylene glycol dimethacrylate-Elements of molecularly imprinted polymer modeling process. *Polymer* 52: 1206-1216.
24. Harwood, L. M., Moody, C. J., and Percy, J. M. (1999). Experimental Organic Chemistry: standard and microscale. 2nd edition. Malden, MA: Blackwell, Science Publishing. 276-305.
25. Xie, C., Liu, B., Wang, Z., Gao, D., Guan, G. and Zhang, Z. (2008). Molecular Imprinting at Walls of Silica Nanotubes for TNT Recognition. *Analytical Chemistry* 80(2): 437-443.